Proceedings of the 3rd International Conference on Fluid Flow, Heat and Mass Transfer (FFHMT'16)
Ottawa, Canada – May 2 – 3, 2016
Paper No. 155

Numerical Simulations of Al_2O_3 Nanofluid Flows in the Laminar and Turbulent Regimes in a Uniformly Heated Pipe

Ghofrane Sekrani[1,2], Sébastien Poncet[2], Mourad Bouterra[1]
[1]LETTM, Faculty of Sciences, University of Tunis – El Manar
Tunis, Tunisia
[2]Mechanical Engineering Department, Université de Sherbrooke
2500 boulevard de l'Université, Sherbrooke, Canada
Ghofrane.sekrani@USherbrooke.ca; Sebastien.Poncet@USherbrooke.ca; mourad.bouterra@fst.rnu.tn

Abstract **-** In the present paper, laminar and turbulent forced convection flows in a horizontal pipe with Al_2O_3-water nanofluid are considered numerically. A single phase model formulation is used for comparison with the mixture model. Temperature-dependent fluid properties are taken into account for all cases. The heat transfer coefficients computed with the mixture model showed a better agreement with experimental data reported in the literature as compared to the single phase model. Temperature-dependent fluid properties result in a better prediction of the thermal field under the effect of a constant heat flux, whereas calculations with constant fluid properties result in an over prediction of the heat transfer coefficient. The results are presented and discussed for six values of the Reynolds number covering the laminar and turbulent flow regimes and four values of the concentration in nanoparticles within the range $0 \leq \phi \leq 2\%$.

Keywords**:** Nanofluid; numerical simulation; heat transfer; Al_2O_3 nanoparticles, laminar flow; turbulence

1. Introduction

Nanofluids are engineered colloids made of a base fluid and nanoparticles (1-100 nm). The term nanofluid was first proposed by Choi and Eastman [1] in 1995. Nanoparticles are relatively close in size to the molecules of the base fluid, and thus can realize very stable suspensions contrary to the milli-and microsized suspensions explored in the past. Researchers have demonstrated an abnormal increase of the nanofluid properties. For example, Eastman et al. [2] reported a 40% increase in the thermal conductivity of ethylene-glycol with 0.3% of copper nanoparticles. Pak and Cho [3] measured a thermal enhancement of about 30% using alumina-water and titania-water nanofluids compared to pure liquid water.

Numerous theoretical and experimental studies have been conducted to determine the thermophysical properties of nanofluids and the best approach to model such mixtures [1, 4-6]. The emphasis was mainly focused on the performances of single phase or two phase approaches. Single phase models use the proper effective properties of nanofluids without taking into account the chaotic motion of the nanoparticles and solve the problem as a unique fluid without any interaction between the phases. The two phase approach is based on an assumption of continuum phases. It provides a field description of the dynamics of each phase or alternatively, the Lagrangian trajectories of individual particles coupled with the Eulerian description of the main flow field. Therefore, the two phase approach appears better to simulate the nanofluid flows and especially the mixture model [6,7]. Akbari et al. [5] showed that the mixture model provides the best trade-off between accuracy and computational cost and performs quite well against the experimental data of Wen and Ding [8].

The objective of the present paper is three-fold: (i) to develop a similar CFD model based on the former work of [5] and extend it to other values of Reynolds number and nanoparticle concentrations in the laminar regime, (ii) to show the importance of the mesh grid distribution and many other numerical parameters on the quality of the predicted heat transfer distribution and (iii) to extend the results and the discussion to the turbulent flow regime considering several values of the Reynolds number and nanoparticle concentration. The experimental set-up developed by Wen and Ding and the numerical simulations of Akbari et al. [5] in the same configuration are used for comparisons and to validate the model in the laminar flow regime. The literature about nanofluids is too abundant for a detail state of the art, such that the reader can refer to the very recent monograph of Bianco et al. [9] for more details.

2. Numerical Approach

2.1. Geometrical Modeling

A horizontal circular pipe of length L=0.97 m and diameter D=2R=0.0045 m is considered in the present work. It corresponds to the experimental set-up developed by Wen and Ding [8]. The nanofluid selected for this study contains 42 nm average size Al_2O_3 nanoparticles dispersed in water as a base fluid. A constant heat flux is imposed at the tube wall.

2.1. Numerical Method

The three-dimensional governing equations for the conservation of mass, momentum and energy and for the single-phase and the mixture models are solved using a finite volume approach. The spatial discretization is achieved through a second-order upwind scheme. The SIMPLEC algorithm is selected to overcome the pressure-velocity coupling. All calculations are steady state and three-dimensional. Unsteady calculations have been also performed leading to similar results. In the turbulent regime, a standard k-ε model is used in its low-Reynolds number formulation.

2.2. Single and Mixture Models

The physical properties of water are considered to be temperature-dependent while those of the solid nanoparticles are kept constant. The following equations are used to evaluate the conductivity, dynamic viscosity [10], density [11] and specific heat [4] of pure liquid water (index f) as a function of temperature T:

$$K_f = -0.76761 + 7.535211 \times 10^{-3}T - 0.98249 \times 10^{-5}T^2 \quad (1)$$

$$\mu_f = 2.414 \times 10^{-5} \times 10^{\left(\frac{247.8}{T-140}\right)} \quad (2)$$

$$\rho_f = 2446 - 20.674T + 0.11576T^2 - 3.12895 \times 10^{-4}T^3 + 4.0505 \times 10^{-7}T^4 - 2.0546 \times 10^{-10}T^5 \quad (3)$$

$$(C_p)_f = \exp\left(\frac{8.29041 - 0.012557T}{1 - 1.52373 \times 10^{-3}T}\right) \quad (4)$$

Two models have been considered to simulate Al_2O_3-water nanofluid in a heated pipe: the single phase model and the mixture model, which are briefly described in the following. All details may be found in [5]. The mixture model assumes a strong coupling between the fluid and solid phases, such that nanoparticles closely follow the flow. Only one set of governing equations for the mixture is solved but a drift velocity between the solid particles and the base fluid is allowed.

The single phase model, which is generally used for nanofluid flows, was implemented for comparison with the mixture model in the laminar regime. This model treats the nanofluid as a homogeneous fluid with effective properties and solves only one set of differential equations for the conservation of mass, momentum and energy applied to this pseudofluid. The nanofluid properties are function of the base fluid and nanoparticles properties given in Table 1 as well as the volume fraction of nanoparticles. The conductivity K_{nf} [12], the dynamic viscosity μ_{nf} [5], the density ρ_{nf} and heat capacity Cp_{nf} [14] of the nanofluid are given by:

$$K_{nf} = K_{bf}(1-\phi) + \gamma K_{np}\phi + C_d \frac{d_{bf}}{d_{np}} K_{bf}\, Re_{np}^2 Pr\phi \quad (5)$$

$$\mu_{nf} = (1 + 0.025\phi + 0.015\phi^2)\mu_{bf} \quad (6)$$

$$\rho_{nf} = (1-\phi)\rho_{bf} + \phi\rho_{np} \quad (7)$$

$$(C_p)_{nf} = \frac{(1-\phi)(\rho C_p)_{bf} + \phi(\rho C_p)_{np}}{\rho_{nf}} \quad (8)$$

where γ=0.01, $C_d=18\times10^{-6}$, Re_{np} is the Reynolds number based on the nanoparticle with a random motion velocity equal to 0.1 m/s, d_{bf}=0.384 nm is the equivalent diameter of a water molecule [13] and Pr=7 the Prandtl number. ϕ denotes

the Al_2O_3 concentration, the index np refers to nanoparticles and bf (or f) to the base fluid. Note that imposing a classical relation C_d=f(Re) leads to undistinguishable results.

Table 1: Thermophysical properties of water and Al_2O_3 nanoparticles after [13].

	ρ (kg/m³)	Cp (J/kg/K)	K (W/m/K)	μ (Pa.s)
Water	998.2	4182	0.6	0.001003
Al_2O_3	3880	729	42	-

2.3. Numerical Details

At the tube inlet, uniform axial velocity V_0 and temperature T_0=293K, are assumed. Moreover, constant intensity turbulence levels equal to 1% are imposed. Several tests have shown that such value has no noticeable influence on the heat transfer distribution within the pipe. At the pipe outlet, a given pressure level is fixed. On the pipe wall, a uniform heat flux of 130 W is imposed with no-slip boundary conditions for the velocity field (u=v=w=0). It corresponds to the experimental conditions considered by Wen and Ding [8].

A structured mesh is used throughout the domain, with 140 nodes in the circumferential direction, 220 in the radial direction and 800 in the axial direction. A grid refinement close to the wall is necessary to ensure a maximum wall coordinate less than unity in the turbulent case. The mesh is also refined at the pipe entrance, where the highest velocity and temperature gradients are reached. This mesh grid provides grid-independent solution for all cases.

3. Laminar Flow Regime

Three different values of the Reynolds number Re=600, 1000 and 1600 and three concentrations in nanoparticles ϕ=0.6, 1 and 1.6% have been considered in the following.

3.1. Validation of the Numerical Model

In order to first validate the numerical model, the local heat transfer coefficient h(z) has been evaluated along the pipe length z. Due to the lack of precise information of how it is measured in the experiments of Wen and Ding [8], four different averaging method have been used to determine the wall temperature in the numerics (see in Figure 1a).

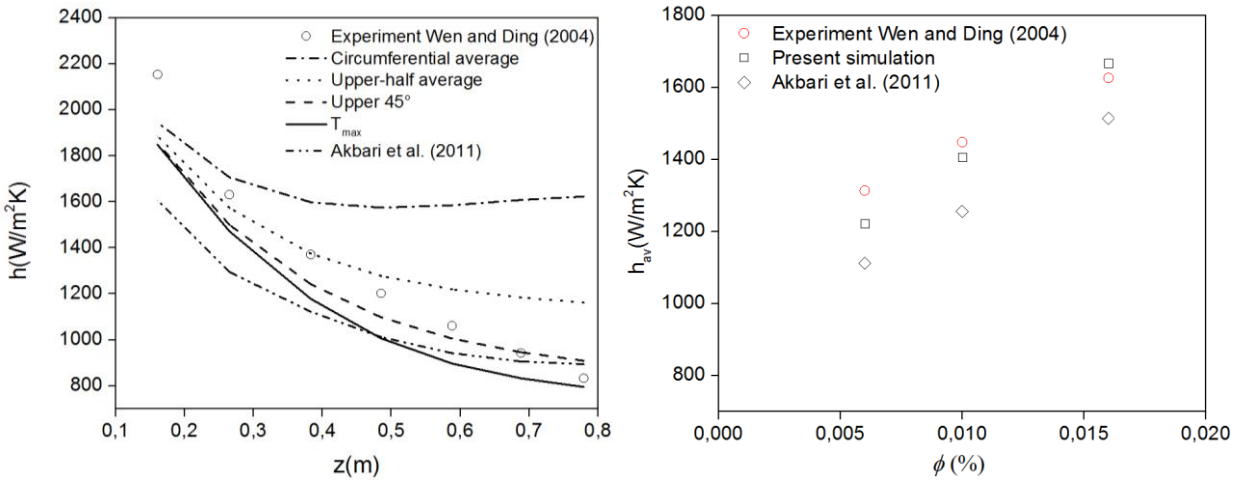

Fig. 1: (a) Local heat transfer coefficient predicted by the mixture model with different ways to evaluate the wall temperature for Re=1600 and ϕ=0.006; (b) Influence of the nanoparticle concentration on the average heat transfer coefficient for Re=1600.

Comparisons have been performed with the measurements of Wen and Ding [8] and the numerical simulations of Akbari et al. [5] for Re=1600 and ϕ=0.6%. A similar procedure has been done by [8] as no sufficient information is provided in the experiments about the evaluation of the heat transfer coefficient. Using an average over an upper arc of +/- 45° leads to closer results compared to the experiments. The same behaviors have been obtained for other combinations of Reynolds number and concentration in nanoparticles. This averaging method will be used in the following. The present

simulations agree particularly well with the experiments [8] with an exponential decrease of the heat transfer coefficient as expected from a simple energy balance. The main discrepancy is observed close to the inlet. It may be explained by the choice of the boundary conditions. The experimental conditions are unknown, such that imposing a constant axial velocity at the inlet was the simplest choice. The present simulations improve the predictions of Akbari et al. [5] using the same solver and methods. It points out in particular the necessity to use an appropriate mesh grid in the near-wall regions.

Figure 1b provides further comparisons in terms of the average heat transfer coefficient for Re=1600 and three values of the concentration in nanoparticles. The present results obtained using the mixture model show an acceptable agreement with the experimental ones. The experimental data show an average enhancement of about 24% with increased alumina nanoparticle concentration from 0.6% to 1.6%. In the numerics, a concentration of 1.6% enhances the heat transfer up to a factor 2 compared to the base case with pure liquid water. Once again, the present simulations improve the previous ones of Akbari et al. [5] pointing out the influence of the mesh grid. The authors used 180 nodes in the axial direction, 40 nodes in the circumferential direction, and 40 nodes in the radial direction, which represent 86 times less mesh points than in the present case.

A comprehensive investigation about the influence of taking into account temperature-dependent properties has been carried out. Figure 2a displays the axial distribution of the local heat transfer coefficient for Re=1600 and four concentrations in nanoparticles. Using temperature-dependent or variable thermophysical properties (VP) [5] leads to very satisfactory results as shown in Figures 1a and 1b. On the contrary, using constant properties (CP) leads to a strong overestimation of the heat transfer coefficient, with more pronounced differences towards the thermally fully developed flow region. In fact, the thermal conductivity of the nanofluid increases drastically with temperature and density decreases. Using VP, the circumferential wall temperature appears to be non-uniformly distributed in the tangential direction, whereas the CP model exhibits a more uniform and axisymmetric behavior. The VP model takes then into account buoyancy effects which result in a noticeable increase of the fluid temperature in the upper half of the pipe. Surprisingly, Labonté et al. [15] found that CP lead to an underestimation of the heat transfer coefficient. This difference might be attributed to the different multiphase models used. Proper empirical correlations to account for the effect of the temperature changes on the fluid properties will be then used in the following.

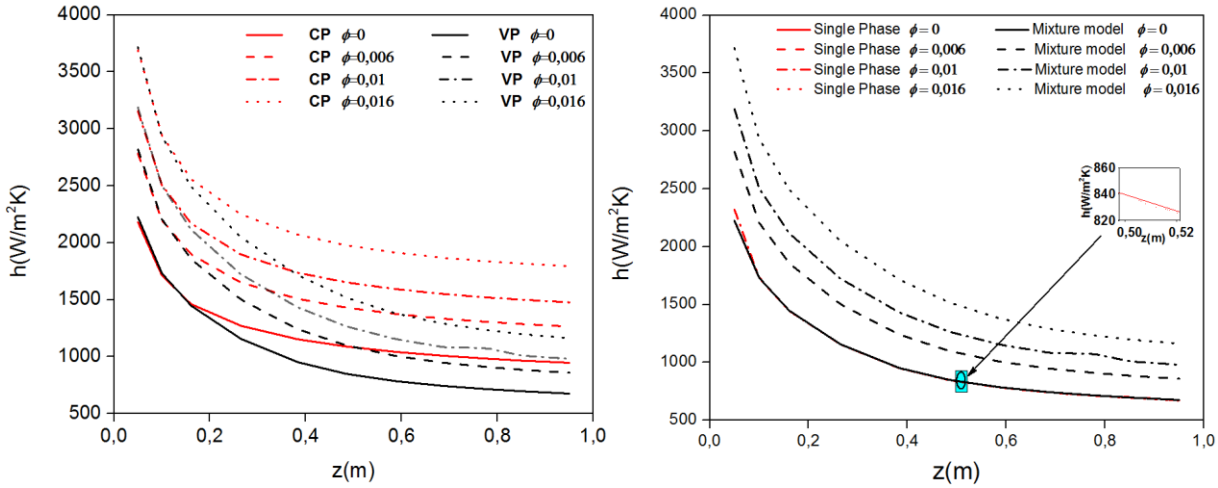

Fig. 2: (a) Effect of constant properties versus variable properties on the axial development of the local heat transfer coefficient for Re=1600; (b) Comparison of calculated axial heat transfer with single phase model and mixture model for Re=1600.

Akbari et al. [5] already showed that Eulerian and Volume of Fluid models do not improve the predictions of the mixture model. Thus, only the single phase and the mixture models have been compared in Figure 2b for Re=1600 and four concentrations in nanoparticles. The single phase model fails to predict the right axial distributions of the local heat transfer coefficient. A smooth decrease with the axial distance is certainly observed but the heat transfer is not improved at all when increasing the concentration in nanoparticles. The results get closer to the ones obtained by the mixture model for ϕ=0 at the end of the pipe but a large underestimation is observed everywhere else. It confirms the former results of Akbari et al. [5]. On the other hand, the heat transfer coefficient predicted by the mixture model clearly increases with the increase of the nanoparticle concentration in agreement with the observations of [5-7]. The superiority of the mixture model may

be easily explained. It guarantees a more accurate treatment of the two-phase mixture, as opposed to the single phase model which does not take into account neither the spatial variations of the distribution in nanoparticles in the base fluid, nor the relative velocity of each phase.

3.2. Influence of the Reynolds Number and the Concentration in Nanoparticles on the Heat Transfer

Figure 3a shows the dependence of the average heat transfer coefficient h_{av} on both the nanoparticle concentration and the axial Reynolds number. It can be clearly observed that h_{av} increases both when increasing either the Reynolds number of the concentration in nanoparticles. For example, for ϕ=0.006, h_{av} is equal to 863.68 (W/m²/K), 1012.92 and 1222.26 for Re=600, 1000 and 1600, respectively. A linear dependency is observed according to ϕ whatever the Reynolds number. Figure 3b clearly shows the thermal enhancement due to the nanoparticles along the pipe. For Re=1600, the heat transfer coefficient ratio h_{nf}/h_{bf} increased by 13% and 34% for ϕ=0.01 and ϕ=0.016, respectively. This ratio is rather constant in the axial direction.

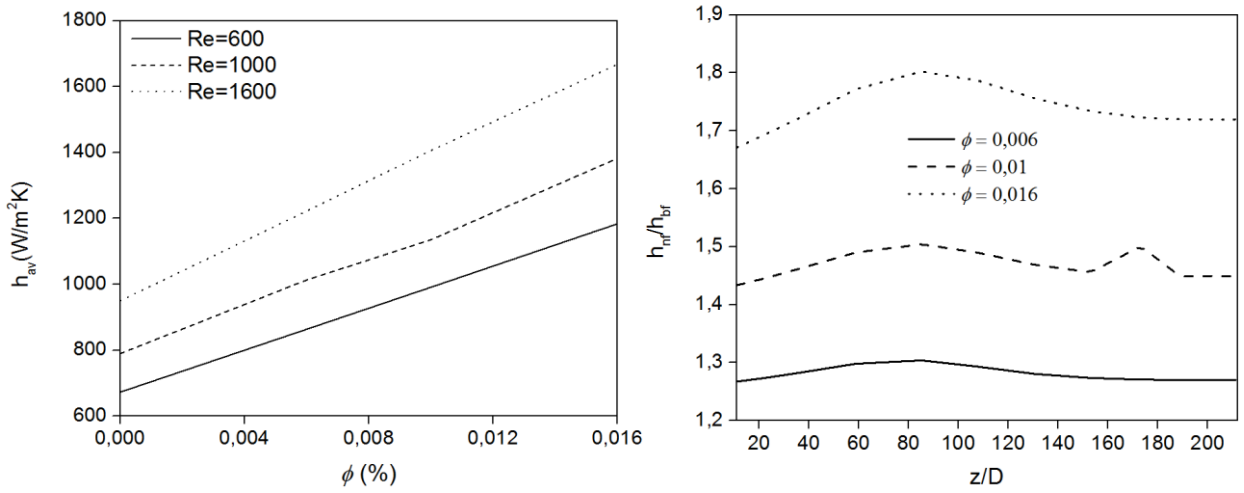

Fig. 3: (a) Effect of the nanoparticle concentration and Reynolds number on the average heat transfer coefficient; (b) Axial variations of the heat transfer coefficient ratio h_{nf}/h_{bf} for Re=1600 and three particle concentrations.

Figure 4a shows the axial distributions of the wall and bulk temperatures for Re=1600 and four concentrations in nanoparticles. Both temperatures increase from the inlet to the outlet of the pipe. One can observe also the strong dependence of the wall temperature T_w on the nanoparticle concentration ϕ. T_w decreases noticeably when ϕ increases. Particularly, the temperature difference at tube exit between the base fluid and the nanofluid with ϕ=0.016 is about 10 K. The same remark can be done for the bulk temperature T_f with only weak variations with ϕ. The difference at the tube outlet between the base case ϕ=0 and a concentration of ϕ=1.6% is around 1 K for this Reynolds number. The presence of nanoparticles and their thermal properties improve noticeably the heat transfer between the heated wall and the base fluid. Additionally, the Brownian motion of the particles plays a significant role in the diffusion of heat inside the base fluid [16].

More interesting is the axial distributions of the nanoparticle concentration along the pipe at different radii. Figure 4b displays the axial profiles of ϕ at r/R=0.98 (top wall), r/R=0 (axis) and r/R=-0.98 (bottom wall) for Re=1600 and an initial concentration of ϕ=1.6%. It is important to note firstly the y-scale remains between 1.575% and 1.625%, such that the variations are rather small and secondly that these values are extracted on a vertical line 0-180° and so do not take into account three-dimensional effects. The first remark is that the concentration is rather constant along the centerline of the pipe and as well as close to the bottom wall. On the contrary, along the top wall of the pipe, the concentration in nanoparticles decrease. The gravity force is highest than the buoyancy one, which leads to a weak sedimentation process. Such phenomenon is one of the two major drawbacks when using nanofluids and explains partly why the difference regarding the heat transfer coefficient is weaker at the tube outlet than close to the inlet.

The hydrodynamic field is not shown here but it can be noticed that with the development and thickening of the boundary layers, the axial velocity at the axis increases when moving towards the outlet of the cavity. A slight decrease is observed between z=0.3 and z=0.6 m due to the appearance of a secondary flow induced by the competition between

gravity and buoyancy forces [5,17,18], which is characteristic of all mixed convection flows. Then, the axial velocity at the centerline reaches an asymptotic value due to the weakening of the secondary flow in the downstream region. The presence of nanoparticles tend to homogenize the mean flow field.

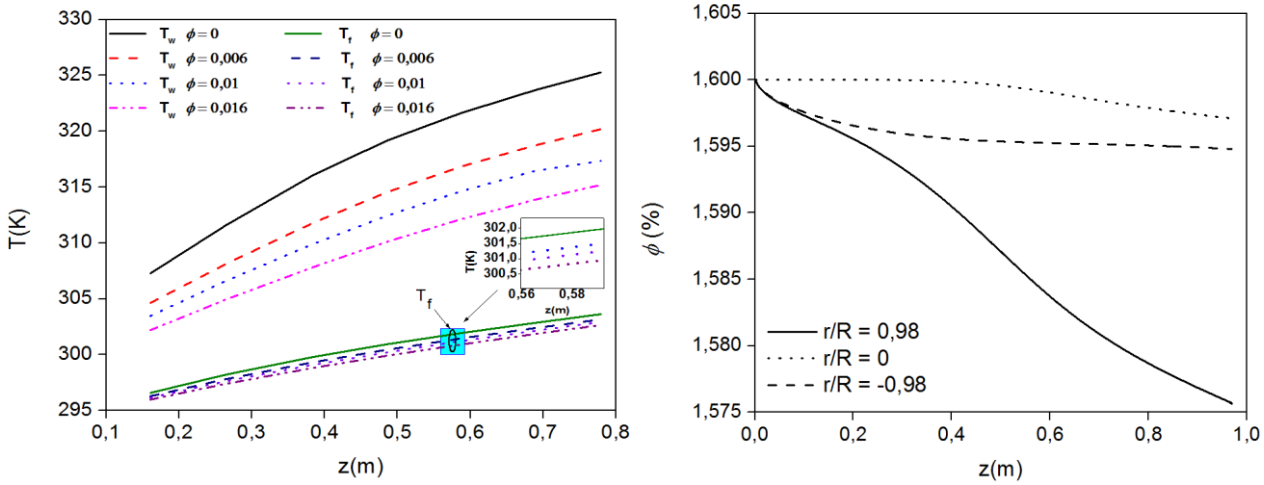

Fig. 4: (a) Axial development of wall and bulk temperatures for Re=1600; (b) Axial distribution of the nanoparticle concentration for Re=1600 and ϕ=0.016.

4. Extension to the Turbulent Flow Regime

The numerical simulations have been extended here to the turbulent flow regime using a standard k-ε model with wall treatment enhancement. As for the laminar regime, three concentrations in nanoparticles have been considered, ϕ=0.6, 1 and 1.6% as well as three values of the Reynolds number, Re=5000, 10000 and 15000. The transition to turbulence in such flow configurations is typically obtained for Re~2000 but also strongly depends on the wall roughness and many other parameters. These values guarantee here to get a fully turbulent flow regime.

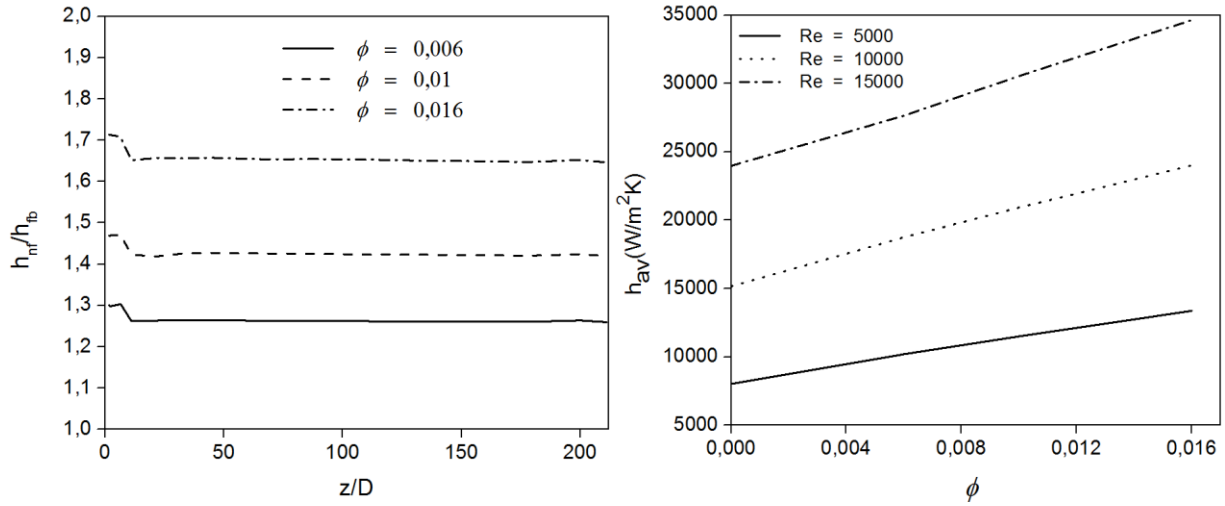

Fig. 5: (a) Axial variations of heat transfer coefficient ratio h_{nf}/h_{bf} for Re =5000 and three nanoparticle concentrations; (b) Influence of the nanoparticle concentration and Reynolds number on the average heat transfer coefficient.

Firstly, the distributions of the local heat transfer coefficient along the pipe are similar to the laminar regime with an exponential decrease with the axial distance z. More interesting is to evaluate the thermal enhancement due to the nanoparticles. Figure 5a shows the distributions of the heat transfer coefficient ratio according to z/D for Re=5000 and three concentrations. The ratio is rather constant along the pipe. Increasing the nanoparticle concentration leads, as

expected, to a better thermal enhancement. A concentration of 1.6% leads to an increase of around 66% in terms of the local heat transfer compared to pure water. This value is slightly lower to that obtained in the laminar case (Figure 3b).

Figure 5b reports the influence of the concentration ϕ on the average heat transfer coefficient for three Reynolds numbers. The coefficient h_{av} increases with increasing values of both Re and ϕ. For example, for ϕ=0.01, it takes the values h_{av}=1199.8 W/m²/K, 20922.1 and 30541 for Re=5000, 10000 and 15000 respectively. Similarly to the laminar regime, a linear dependency with ϕ is observed.

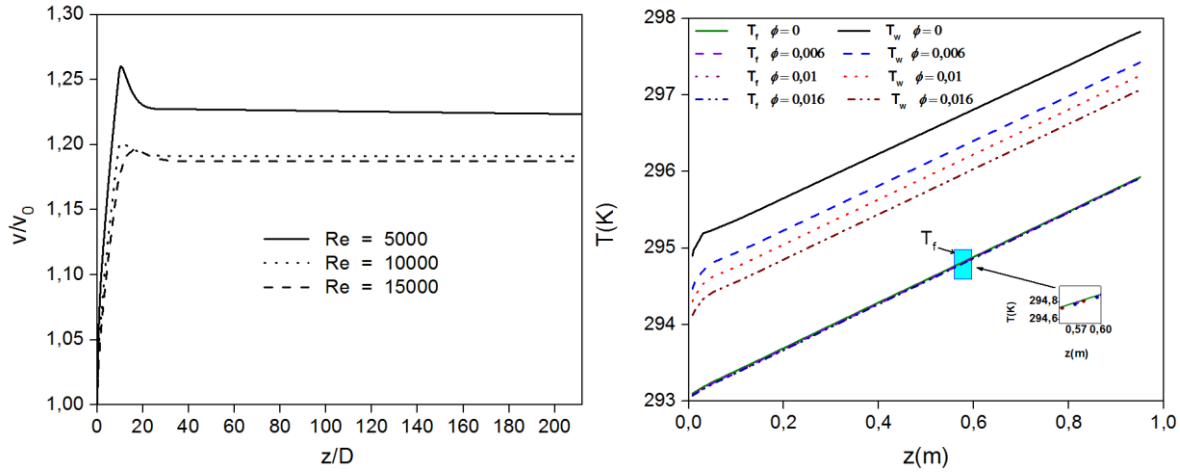

Fig. 6: (a) Axial variations of the axial mean velocity at r/R=0 for ϕ=0.016; (b) Axial development of the wall and bulk temperatures for Re=5000 and four concentrations in nanoparticles.

The axial evolutions of the axial velocity along the tube centerline for ϕ=0.016 is shown in Figure 6a. The velocity distributions suggest the existence of a fully developed region starting from z/D=30 for all values of the Reynolds numbers as already observed in the laminar regime. In accordance with [4,7], immediately after the tube inlet, the boundary layer growth tends to push the fluid towards the axis region, causing an increase of the axial velocity. The turbulent mixing results in a more uniform velocity distribution in the fully developed region. It is interesting to note that the centerline velocity decreases as the Reynolds number increases. The increase of the nanoparticle concentration has no significant effect on the mean axial velocity and so is not shown here.

Figure 5b exhibits the axial distributions of the wall and bulk temperatures for Re=5000 and four concentrations. The profiles show that the addition of nanoparticles clearly affects the wall temperature, with a noticeable decrease with the increase of the nanoparticle concentration. Unlike the laminar case, the difference in terms of the wall temperature between the base fluid and the nanofluid at the tube exit for Re=5000 and ϕ=0.016 is estimated to be 1 K, and the difference in the bulk temperature remains less than 0.08 K. Both temperatures increase linearly with z.

5. Conclusion

Laminar and turbulent nanofluid flows in a horizontal heated tube have been simulated for a wide range of Reynolds numbers [600-15000] and different values of the nanoparticle concentration [0.6-1.6%]. The nanofluid is composed of Al_2O_3 nanoparticles and liquid water as the base fluid. This work is an extension of the previous numerical study of Akbari et al. [5], while the geometry and boundary conditions correspond to the experimental set-up of Wen and Ding [8].

Single-phase and mixture models with constant and variable thermophysical properties have been compared to the experimental data of Wen and Ding [8] and to the numerical simulations of Akbari et al. [5]. The mixture model with temperature-dependent thermophysical properties performs best with a close agreement against the experiments. The mesh grid arrangement is crucial to simulate such complex flows, which explains why the present results improve the predictions of Akbari et al. [5] using the same solver and two-phase model.

The introduction of Al_2O_3 nanoparticles clearly enhances the heat transfer all over the tube compared to the base case with pure liquid water. For a given concentration of 1.6%, the heat transfer coefficient increases by a factor 2 in the laminar regime (Re=1600), which is to be compared to an increase of 66% in the turbulent regime (Re=5000).

Further calculations are now required to select the best turbulence models, going towards progressively to large eddy simulations at higher Reynolds numbers. Experimental measurements on the thermophysical properties of Al_2O_3-water

nanofluid are also in progress to try improving the correlations used here for the conductivity, dynamic viscosity, density and specific heat against temperature.

Acknowledgements

The authors would like to thank the NSERC chair on industrial energy efficiency established at Université de Sherbrooke in 2014 and supported by Hydro-Québec, CanmetEnergy and Rio Tinto Alcan. Calculations have been performed using the supercomputer Mammouth Parallèle 2 of Calcul Québec.

References

[1] S. U. S. Choi, J. A. Eastman, "Enhancing thermal conductivity of fluids with nanoparticles," in *Proc. of 1995 ASME Int. Mech. Eng. Congress & Exposition*, San Francisco, 1995.

[2] J. A. Eastman, S. U. S. Choi, S. Li, W. Yu, and L. J. Thompson, "Anomalously increased effective thermal conductivities of ethylene glycol-based nanofluids containing copper nanoparticles," *Appl. Phys. Lett.*, vol. 78, no. 6, pp. 718-720, 2001.

[3] B. C. Pak and Y. I. Cho, "Hydrodynamic and Heat Transfer Study of Dispersed Fluids With Submicron Metallic Oxide Particles," *Exp. Heat Transf.*, vol. 11, no. 2, pp. 151-170, 1998.

[4] A. Behzadmehr, M. Saffar-Avval, and N. Galanis, "Prediction of turbulent forced convection of a nanofluid in a tube with uniform heat flux using a two phase approach," *Int. J. Heat Fluid Flow*, vol. 28, no. 2, pp. 211-219, 2007.

[5] M. Akbari, N. Galanis, and A. Behzadmehr, "Comparative analysis of single and two-phase models for CFD studies of nanofluid heat transfer," *Int. J. Therm. Sci.*, vol. 50, no. 8, pp. 1343-1354, 2011.

[6] R. Lotfi, Y. Saboohi, and A. M. Rashidi, "Numerical study of forced convective heat transfer of Nanofluids: Comparison of different approaches," *Int. Commun. Heat Mass Transf.*, vol. 37, no. 1, pp. 74-78, 2010.

[7] V. Bianco, O. Manca, and S. Nardini, "Numerical investigation on nanofluids turbulent convection heat transfer inside a circular tube," *Int. J. Therm. Sci.*, vol. 50, no. 3, pp. 341-349, 2011.

[8] D. Wen and Y. Ding, "Experimental investigation into convective heat transfer of nanofluids at the entrance region under laminar flow conditions," *Int. J. Heat Mass Transf.*, vol. 47, no. 24, pp. 5181-5188, 2004.

[9] V. Bianco, O. Manca, S. Nardini and K. Vafai, *Heat Transfer Enhancement with Nanofluids*. New-York, CRC Press, Taylor & Francis, 2015.

[10] C. A. Nieto de Castro, S. P. Y. Li, A. Nagashima, R. D. Trengove and W. A. Wakeham, "Standard reference data for the thermal conductivity of liquids," *J. Phys. Chem. Ref. Data*, vol. 15, no. 3, pp. 1073-1086, 1986.

[11] R. C. Reid, *Tables on the Thermophysical Properties of Liquids and Gases*. New-York, Halsted Press, 1975.

[12] C. H. Chon, K. D. Kihm, S. P. Lee, and S. U. S. Choi, "Empirical correlation finding the role of temperature and particle size for nanofluid (Al_2O_3) thermal conductivity enhancement," *Appl. Phys. Lett.*, vol. 87, pp. 153107, 2005.

[13] S. P. Jang and S. U. S. Choi, "Effects of Various Parameters on Nanofluid Thermal Conductivity," *J. Heat Transfer*, vol. 129, no. 5, pp. 617-623, 2007.

[14] K. Khanafer, K. Vafai, and M. Lightstone, "Buoyancy-driven heat transfer enhancement in a two-dimensional enclosure utilizing nanofluids," *Int. J. Heat Mass Transf.*, vol. 46, no. 19, pp. 3639-3653, 2003.

[15] J. Labonté, C. T. Nguyen, and G. Roy, "Heat Transfer Enhancement in Laminar Flow Using Al_2O_3-Water Nanofluid Considering Temperature-Dependent Properties," in *Proc. of 4th WSEAS Int. Conf. Heat Transf. Therm. Eng. Environ.*, Elounda, Greece, pp. 331–336, 2006.

[16] M. R. Azizian, H. Ş. Aybar, and T. Okutucu, "Effect of nanoconvection due to Brownian motion on thermal conductivity of nanofluids," *Proc. 7th IASME / WSEAS Int. Conf. Heat Transf. Therm. Eng. Environ.*, pp. 53-56, 2009.

[17] M. Ouzzane and N. Galanis, "Developing Mixed Convection in an Inclined Tube With Circumferentially Nonuniform Heating At Its Outer Surface," *Numer. Heat Transf. Part A*, vol. 35, no. 6, pp. 609-628, 1999.

[18] M. Akbari and A. Behzadmehr, "Developing mixed convection of a nanofluid in a horizontal tube with uniform heat flux," *Int. J. Numer. Methods Heat Fluid Flow*, vol. 17, no. 6, pp. 566-586, 2007.